GEOMETRY CLOSURE FOR HEMODYNAMICS SIMULATIONS

J. Bruijns
Philips Research, High Tech Campus 36, 5656 AE, Eindhoven, The Netherlands

R. Hermans
Philips Healthcare, Veenpluis 8, 5684 PC, Best, The Netherlands

Keywords: 3D rotational angiography, Computer assisted diagnosis, Hemodynamics simulations.

Abstract: Physicians may treat an aneurysm by injecting coils through a catheter into the aneurysm, or by anchoring a stent as a flow diverter. Since such an intervention is risky, a patient is only treated when the probability of aneurysm rupture is relatively high. Hemodynamic properties of aneurysmal blood flow, extracted by computational fluid dynamics calculations, are hypothesized to be relevant for predicting this rupture. Since hemodynamics simulations require a closed vessel section with defined inflow and outflow points, and since the user can easily overlook small side branches, we have developed an algorithm for fully-automatic geometry closure of an open vessel section. Since X-ray based flow returns an indication for the needed length to have a developed flow inside the geometry, we have also developed an algorithm to create a geometry closure around an aneurysm based on a length criterion. After both geometry closure algorithms were tested elaborately, practicability of the hemodynamics workstation is currently being tested.

1 INTRODUCTION

Volume representations of blood vessels acquired by 3D rotational angiography after injection with a contrast agent (Moret et al., 1998) have a clear distinction in gray values between tissue and vessel voxels. Therefore, these volume representations are very suitable for diagnosing an aneurysm, a local widening of a vessel caused by a weak vessel wall (see Figure 1).

Physicians may treat an aneurysm by first moving a catheter inside the aneurysm and next injecting coils through the catheter into the aneurysm. An alternative that is becoming increasingly popular is using a stent as a flow diverter. Since such an intervention is risky, a patient is only treated when the probability of aneurysm rupture is relatively high. So, it is very important to be able to estimate the probability of aneurysm rupture (see also www.aneurist.org). Hemodynamic properties of aneurysmal blood flow are hypothesized to be relevant for predicting this rupture.

Since hemodynamics simulations (i.e. computational fluid dynamics calculations using for example finite element methods) gives highly detailed results in space and time of wall shear stress, pressure, flow impact regions, vorticity and "turbulent" flow, hemodynamics simulations can be used to assess the risk of an aneurysm rupture (Butty et al., 2002; Venugopal et al., 2005; Cebral et al., 2005; Castro et al., 2005).

Figure 1: An aneurysm inside the white rectangle.

The points where blood is flowing into the ge-

Bruijns J. and Hermans R. (2009).
GEOMETRY CLOSURE FOR HEMODYNAMICS SIMULATIONS.
In *Proceedings of the Fourth International Conference on Computer Vision Theory and Applications*, pages 153-161
DOI: 10.5220/0001782701530161

ometry and out of the geometry can be selected by the user or derived from X-ray based flow (Waechter et al., 2008). The user may not have selected all points needed to close the geometry; therefore, we have developed an algorithm for fully-automatic geometry closure of an open vessel section. The basic hypothesis of our algorithm is that the vessel branches on the shortest paths between the selected points are members of the flow section. Connections between these member branches and the other vessel branches which are not marked by the user as either an inflow or an outflow point (i.e. unintentional open connections), are closed by a blockade (further details are given in Section 4).

X-ray based flow returns amongst other things an indication for the needed length to have a developed flow inside the geometry. Therefore, we have developed also an algorithm to create a geometry closure around an aneurysm based on a length criterion. First, a blockade is created at those points of the vessel branches for which the shortest path distance to the aneurysm is equal to this length. In a second step, a blockade is created at those extremities of the vessels for which the shortest path distance to the aneurysm is less than this length (described in Section 5).

We have used 48 clinical volume datasets with an aneurysm to test both geometry closure algorithms elaborately (reported in Section 7).

2 RELATED WORK

In 2006 the European funded Aneurist project was started (www.aneurist.org). This project has the goal to provide an integrated decision support system to assess the risk of cerebral aneurysm rupture in patients and to optimize their treatments. Hemodynamics simulations on patient specific aneurysm is a part of this.

Hemodynamics simulations is a topic of increasing interest. Major advances towards clinical relevance and applicability have been made by dr. J. Cebral of the department of computational and data sciences of George Mason University, USA, VA.

Advances in flow assessment directly from the X-ray images has been made in the work of I. Waechter (Waechter et al., 2008).

3 PREAMBLE

Our starting point is a segmented volume with tissue voxels, aneurysm voxels and “normal” vessel voxels (Bruijns et al., 2007), and the set of directed graphs (one for each component of the voxel vessel structures) with nodes (one for each vessel junction, one for each vessel extremity and one for each aneurysm neck; nodes at the aneurysm necks are called *“neck nodes”*) and skeleton branches (one for each vessel branch) (Bruijns, 2001). A skeleton branch consists of a set of face connected vessel voxels, called *“skeleton voxels”*. The skeleton voxels, located close to the center line of the vessel branch, have a unique label per vessel branch. An example is shown in Figure 2.

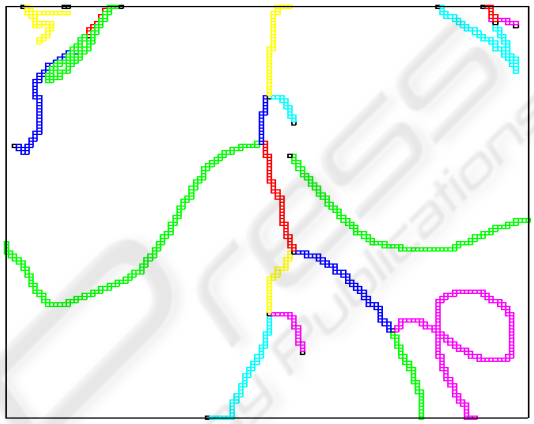

Figure 2: The skeleton voxels of the graphs.

The skeleton voxels are displayed in a color according to their label but skeleton voxels with different labels can have the same color because of the limited number of colors used for display.

The nodes are equipped with geometry (see Figure 3). A center sphere together with the center planes give the position, the size and the delineation of the center region (i.e. the junction). The branch spheres together with the branch planes give the size and the direction of the branch regions adjacent to the center region.

4 FULLY-AUTOMATIC GEOMETRY CLOSURE OF AN OPEN VESSEL SECTION

Hemodynamics simulations are only possible when all points where blood is flowing into the geometry and out of the geometry are known. The user can select the vessel section (called *“flow section”* from now on) by launching a series of probes (Bruijns et al., 2005) on to the vessel branches (see Figure 4). The plane of such a boundary probe separates the vessel voxels at one side of the plane from the vessel voxels at the other side of the plane. If the normal of this plane is pointing into the intended flow section,

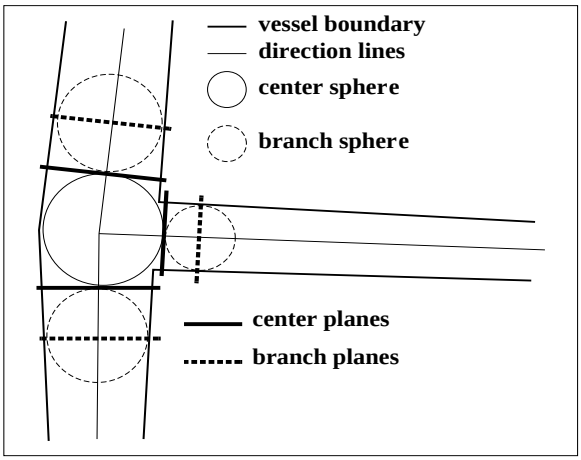

Figure 3: The node geometry.

the vessel voxels at the positive side of the plane are members of the flow section and the vessel voxels at the negative side not.

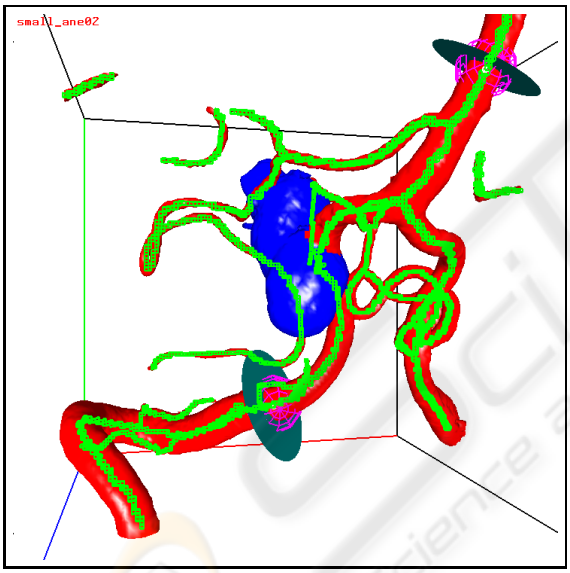

Figure 4: Initial boundary probes; the skeleton voxels are green; the aneurysm part is blue.

Our program connects each boundary probe to a skeleton voxel. The corresponding skeleton voxel is called a *"boundary skeleton voxel"*. Since the closure of a flow section can be checked more easily when a boundary skeleton voxel has exactly two face neighbor skeleton voxels (will be given further detail in Section 6), and since the first and last skeleton voxel of a skeleton branch has either one or more than two face neighbor skeleton voxels, boundary probes are connected to a skeleton voxel between the first and last skeleton voxel of a skeleton branch (changing the position of the probe slightly if necessary).

Since the user can easily forget small side branches, a possible open flow section (i.e. a flow section with not all skeleton branches delimited by a probe as shown in Figure 4) can be closed fully-automatically by the following algorithm:

1. Mark all skeleton voxels of the shortest paths, possibly through the aneurysm, between each pair of boundary probes as member of the flow section.

   The algorithm to compute the shortest path through the aneurysm is similar as the algorithm to compute the path for a connection tube (Bruijns et al., 2005).

   The basic hypothesis of our algorithm is that the skeleton voxels on the shortest paths are members of the flow section. Figure 5 is an example. The black skeleton voxels are located on the shortest paths and thus members of the flow section, the green skeleton voxels are not (yet) members of the flow section. Note that some of the green skeleton voxels are located in the intended flow section.

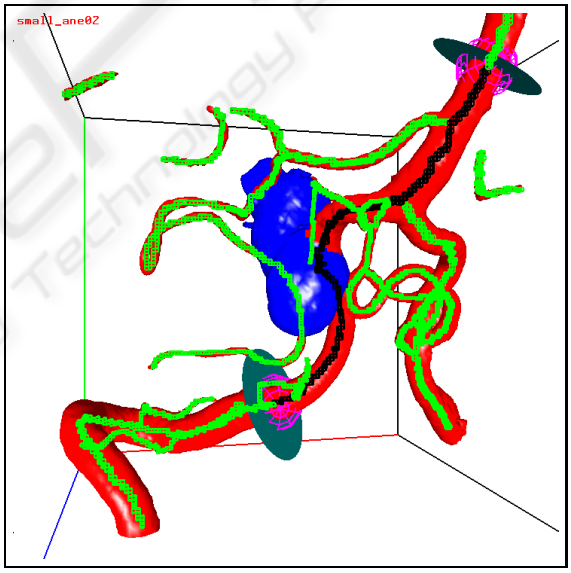

Figure 5: The skeleton voxels of the shortest paths are black, the other skeleton voxels are green.

2. Mark the open vessel nodes type 1.

   After the first step the nodes, located on the shortest paths, have at least one skeleton branch from which the skeleton voxel closest to this node is a member of the flow section (such a skeleton branch is called a *"member branch"* for this node). If such a node has also a skeleton branch from which the skeleton voxel closest to this node is not a member of the flow section (such a skeleton branch is called a *"non-member branch"* for this node), the flow section is open along that

skeleton branch (i.e. there is no boundary probe between a member skeleton voxel and a non-member skeleton voxel).

In some cases, a neck node (see Section 3), not located on the shortest paths, is connected via a very short skeleton branch to an open vessel node type 1 (i.e. the center spheres of the two nodes overlap). In such a case, the aneurysm borders on the flow section. Therefore, such a neck node is also marked as an open vessel node type 1, and the skeleton voxels of the short skeleton branch are marked as member of the flow section. After this procedure, one or both nodes may be no longer an open vessel node type 1 (i.e. all its skeleton branches are member branches), but that is taken care of during the creation of extra boundary probes further on.

3. Mark the open vessel nodes type 2.

   If a neck node is a member of the flow section, there will be no boundary probe between the intended flow section and the aneurysm: the aneurysm is member of the intended flow section (i.e. the skeleton voxels of the neck nodes are conceptually face connected via the aneurysm). In this case, boundary probes are required around the neck nodes which are not located on the shortest paths, to close the flow section.

4. Create and launch boundary probes on the non-member branches of the open vessel nodes type 1, just outside the center sphere. Mark all skeleton voxels along the non-member branches between open vessel nodes type 1 and the corresponding boundary probe as member of the flow section.

   Since the new boundary probe is placed just outside the center sphere of the current node, the skeleton voxels and thus the neighbor vessel voxels, located in the flow section, become members of the flow section.

   Examples of extra boundary probes are shown in Figure 6. Comparing Figure 5 with Figure 6 reveals the extra black skeleton voxels on the skeleton branches which are now also members of the flow section.

5. Create and launch boundary probes on the skeleton branches of the open vessel nodes type 2, as close as possible to the node.

   Since all skeleton branches of an open vessel node type 2 are not members of the flow section, boundary probes has to be placed on each skeleton branch so that the hemodynamics simulations cannot “escape” through the aneurysm to other vessel parts.

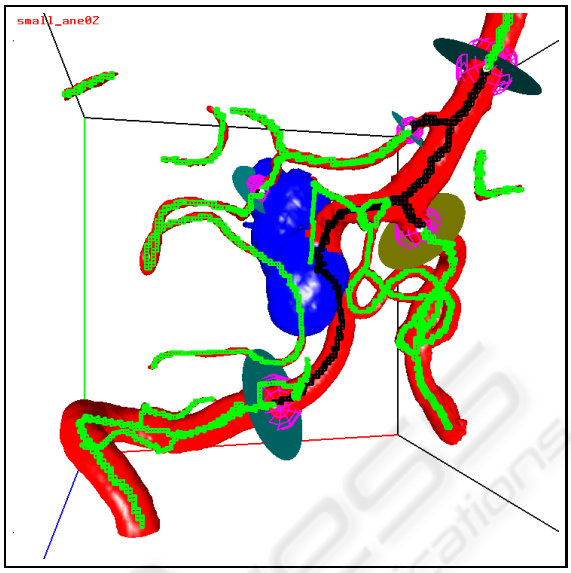

Figure 6: The closed flow section. The skeleton voxels of the flow section are black, the other skeleton voxels are green.

Examples of such boundary probes are shown in Figure 6 at the top of the aneurysm, and more clearly in Figure 7.

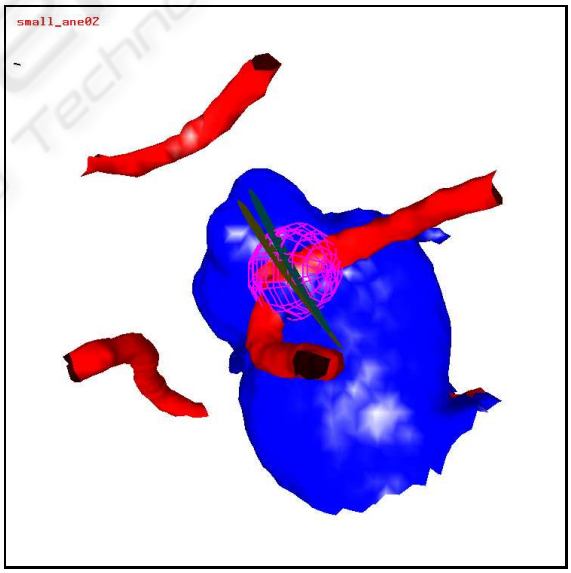

Figure 7: The boundary probes at a neck, not on the shortest paths.

Remarks:

1. The initial boundary probes are created by the user either as inflow or as outflow probes. The extra boundary probes are created by our algorithm as blocking probes. Afterwards, the user can mark

the extra boundary probes as an inflow or an outflow probe. After the user has finished possible adjustments, the vessel is completely closed at the remaining blocking probes by an extra surface mesh.

2. In some cases two open vessel nodes type 1 are connected by a very short non-member branch. In this case, no extra boundary probes are created and all skeleton voxels of such a branch are marked as members of the flow section.
3. In some cases two open vessel nodes type 1 are connected by two paths (i.e. there is a cycle in the vessel graph as shown in Figure 8). Our algorithm selects only the shortest of these two paths (called the *"primary path"*). The other path (called the *"secondary path"*) will be blocked by two blocking probes at the begin and at the end of this path. If the user wants to include also the secondary path and if this secondary path is only slightly longer than the primary path (top case in Figure 8), application of our algorithm to the extended probe configuration (i.e. the extra blocking probes become now initial boundary probes) will include the secondary path because the shortest path between the two blocking probes will run along the secondary path. If the secondary path is too long (i.e. if the shortest path between the two blocking probes runs also along on the primary path; bottom case of Figure 8) the secondary path can be included by launching an extra probe on to the secondary path.

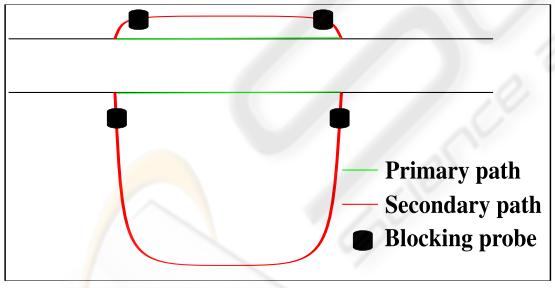

Figure 8: Geometry closure for two cycle cases.

5 FULLY-AUTOMATIC GEOMETRY CLOSURE OF AN ANEURYSM

X-ray based flow helps to estimate amongst other things an indication for the needed length to have a developed flow inside the geometry (Waechter et al., 2008). Therefore, we have developed an algorithm to create a geometry closure around an aneurysm based on a length criterion (i.e. a path distance in face connected voxels). This algorithm consists of the following steps:

1. Compute for each node the shortest path distance to the aneurysm (i.e. to the closest neck node).
2. Launch a blocking probe to each skeleton branch for which the path distance of one node is less than or equal to the needed length and the path distance of the other node is greater than the needed length. Traveling along this skeleton branch, the probe is connected to the first skeleton voxel for which the path distance is greater than or equal to the needed length. Since a boundary skeleton voxel should be located between the first and last skeleton voxel of a skeleton branch, the second skeleton voxel is used when the first skeleton voxel fulfills the distance condition, and the last but one is used when the last skeleton voxel fulfills the distance condition.
3. Launch a blocking probe to each skeleton branch for which one node is an extremity node with a path distance less than or equal to the needed length. The second skeleton voxel counted from the extremity node is used as boundary skeleton voxel.

An example of a small flow section around an aneurysm is shown in Figure 9 and of a large flow section in Figure 10.

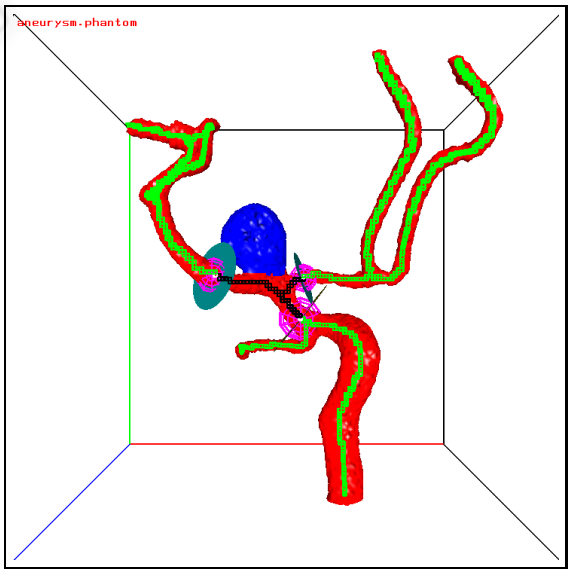

Figure 9: A small flow section around an aneurysm. The skeleton voxels of the flow section are black, the other skeleton voxels are green.

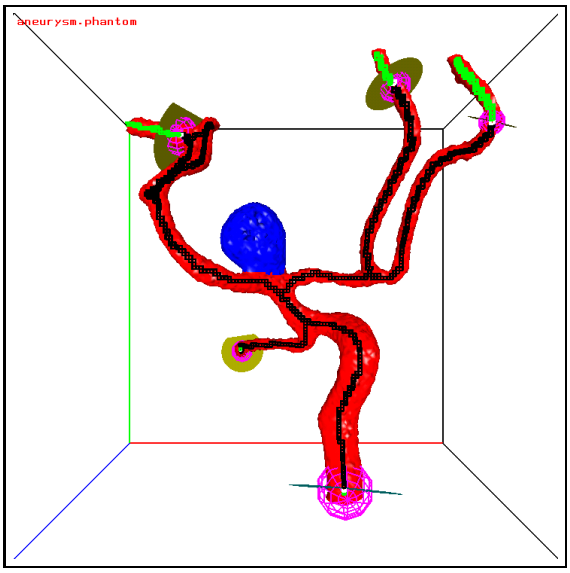

Figure 10: A large flow section around an aneurysm. The skeleton voxels of the flow section are black, the other skeleton voxels are green.

Remark:

In some cases, small side branches should be ignored in the hemodynamics simulations. In that case, this algorithm should be adapted. It may be done as follows. Instead of pure path distances a kind of path expenses should be used. These path expenses are the accumulated branch expenses along the "minimum" path. The branch expenses of small side branches (e.g. diameter less than a user defined value) are set to a very high value. The branch expenses of the other branches are set to the path distance of the branch.

6 VERIFICATION

6.1 Detection of an Open Flow Section

As already mentioned in Section 4, the boundary skeleton voxels to which the boundary probes are launched, are located between the first and last skeleton voxel of a skeleton branch. So, each boundary skeleton voxel has exactly two face neighbor skeleton voxels, one located at the positive side and one located at the negative side of the probe's plane. The closure of the flow section will be verified by looking at the membership of these two face neighbor skeleton voxels. The membership of a skeleton voxel can be computed by the following labelling algorithm:

1. Mark all skeleton voxels with the label "FLOW_IN", indicating that they are as yet member of the flow section.
2. Mark the boundary skeleton voxels with the label "FLOW_BLOCK", indicating that labelling should not be continued across this skeleton voxel.
3. Mark all skeleton voxels at the extremity nodes with the label "FLOW_OUT", indicating that they are not member of the flow section.
4. Mark all skeleton voxels, labelled with the label "FLOW_IN", face connected to a skeleton voxel with the label "FLOW_OUT", with the label "FLOW_OUT", indicating that they are no longer member of the flow section. This step is repeated until no skeleton voxels are changed anymore.

   As mentioned in Section 4, the skeleton voxels of the neck nodes are conceptually face connected via the aneurysm. Therefore, if one of the neck nodes (i.e. its skeleton voxel) is marked with the label "FLOW_OUT", all neck nodes are marked with the label "FLOW_OUT".

A possible open flow section is detected by comparing the face neighbor skeleton voxels of the boundary skeleton voxels. A flow section is open if and only if both face neighbor skeleton voxels have the label "FLOW_OUT", indicating that both skeleton voxels are not a member of the flow section.

Remarks:

1. This verification procedure is used both for checking whether the geometry closure algorithm described in Section 4 has to be executed and for checking whether the selected geometry closure algorithm (i.e. the one described in Section 4 or the one described in Section 5) resulted in a closed flow section.
2. After the labelling algorithm is finished, possible internal probes are removed (just before checking whether the flow section is open or closed). An internal probe is a probe for which both face neighbor skeleton voxels are member of the flow section. An example of a set of initial boundary probes with one internal probe is shown in Figure 11. The closed flow section is shown in Figure 12. The final flow section with the internal probe removed is shown in Figure 13.

6.2 Detection of Multiple Flow Sections

After possible internal probes have been removed and the geometry closure of the flow section has been verified, verification of the number of components of the flow section can be performed. After all, for hemodynamics simulations the flow section should consist of a single connected component.

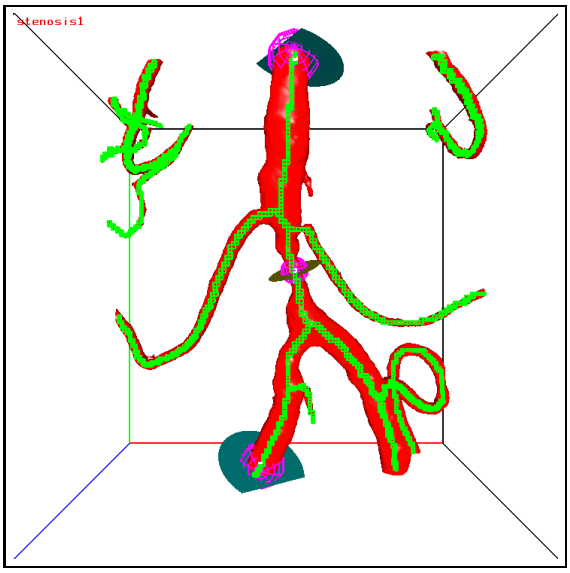

Figure 11: Initial boundary probes with one internal probe. The skeleton voxels are green.

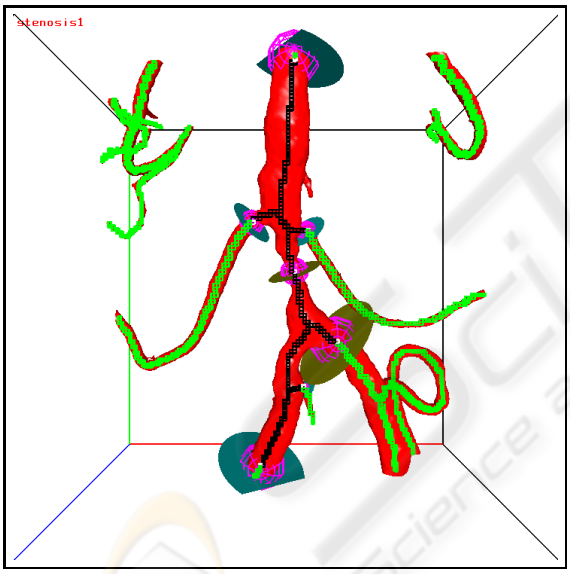

Figure 12: The closed flow section for the internal probe case. The skeleton voxels of the flow section are black, the other skeleton voxels are green.

Checking whether the flow section consists of a single connected component is also performed by a labelling algorithm:

1. Mark all boundary skeleton voxels with the label "FLOW_IN".
2. Mark the first boundary skeleton voxel with the label "FLOW_FIRST".
3. Mark all skeleton voxels, labelled with the label "FLOW_IN", face connected to a skeleton voxel with the label "FLOW_FIRST", with the label "FLOW_FIRST". This step is repeated until no skeleton voxels are changed anymore.

   As mentioned in Section 4, the skeleton voxels of the neck nodes are conceptually face connected via the aneurysm. Therefore, if one of the neck nodes (i.e. its skeleton voxel) is marked with the label "FLOW_FIRST", all neck nodes are marked with the label "FLOW_FIRST". So, two flow sections connected to an aneurysm are considered a single connected component.
4. Check whether all boundary skeleton voxels have the label "FLOW_FIRST".

   If so, the flow section consist of a single connected component.

An example of two separated closed flow sections is shown in Figure 14.

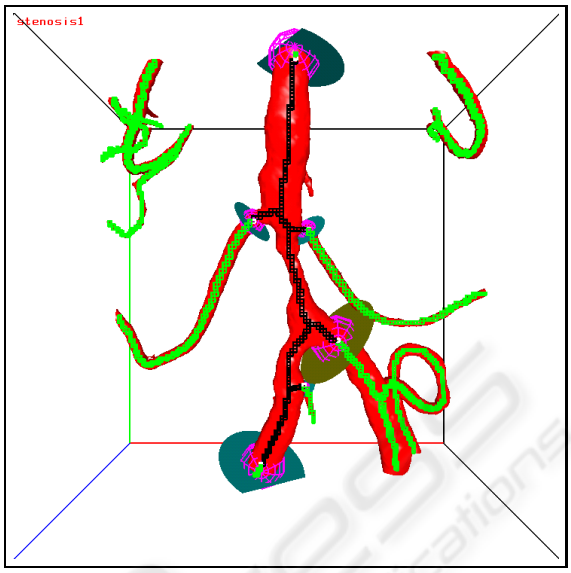

Figure 13: The flow section with the internal probe removed. The skeleton voxels of the flow section are black, the other skeleton voxels are green.

7 EXPERIMENTS AND RESULTS

7.1 For Geometry Closure of an Aneurysm

We have applied the method for fully-automatic geometry closure of an aneurysm (see Section 5) to 48 clinical volume datasets with an aneurysm (15 of them with a resolution of 256x256x256 voxels, the rest 128x128x128 voxels), acquired with the 3D Integris system (Philips-Medical-Systems-Nederland,

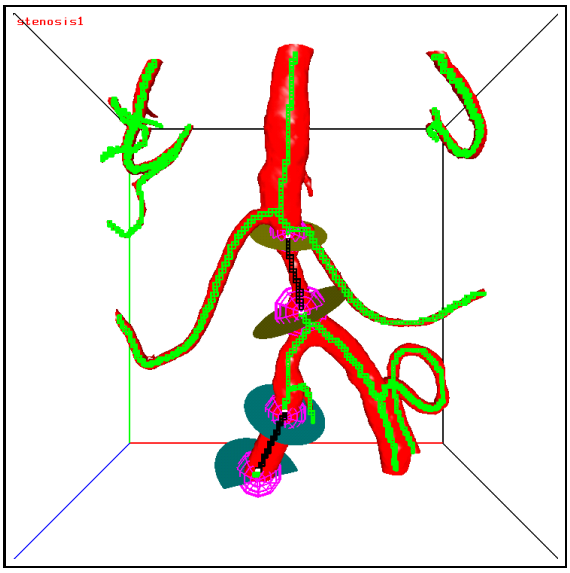

Figure 14: Two separated closed flow sections. The skeleton voxels of the flow sections are black, the other skeleton voxels are green.

2001). The voxel size varies between 0.2 and 1.2 millimeter. We have tested three lengths (path distances in face connected voxels): 31, 101 and 171. Examples are shown in Figure 9 and Figure 10.

Table 1: The characteristics of the number of blocking probes, created by fully-automatic geometry closure of 48 aneurysms, for three different lengths (i.e. path distances in face connected voxels).

Length:	31	101	171
min.	2.0	2.0	3.0
median	4.0	8.0	11.5
mean	4.3	9.1	13.7
max.	11.0	24.0	36.0

The characteristics of the number of blocking probes, created by fully-automatic geometry closure of 48 aneurysms, for these three lengths, are given in Table 1. The characteristics of the elapsed times in seconds are given in Table 2. The elapsed times for the 256x256x256 volumes are divided by 2 to compensate for the on average two times longer path distances. As is clear from this table, the elapsed times are increasing for larger lengths.

After the blocking probes are created, the flow section is checked with the verification algorithms, described in Section 6. For all cases, the flow section was a single connected closed flow section.

Table 2: The characteristics of the elapsed times in seconds for fully-automatic geometry closure of 48 aneurysms, for three different lengths.

Length:	31	101	171
min.	0.016	0.020	0.024
median	0.052	0.103	0.163
mean	0.064	0.119	0.173
max.	0.200	0.304	0.416

7.2 For Closure of an Open Flow Section

We have applied the method for fully-automatic geometry closure of an aneurysm also to generate tests for geometry closure of an open flow section (see Section 4). Indeed, if the required length is set to a very large number, blocking probes will be generated at the extremity nodes of the vessel graph(s) connected to the aneurysm. An example of the generated extremity probes is shown in Figure 15.

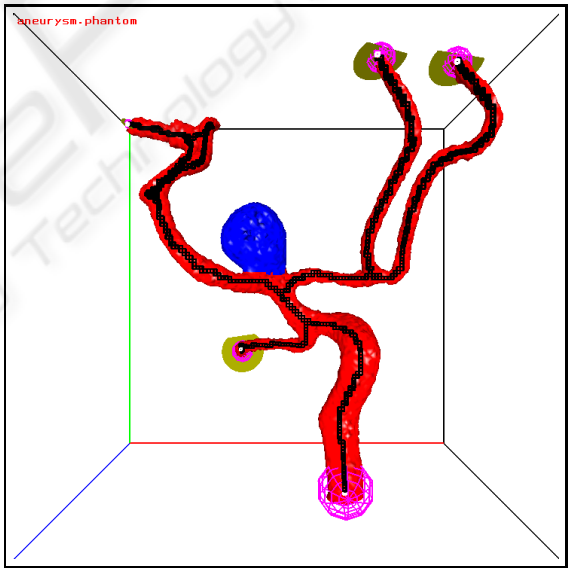

Figure 15: The extremity probes.

We have used each pair of the generated extremity probes as initial boundary probes. An example of the generated blocking probes for two of the initial boundary probes is shown in Figure 16.

The characteristics of the number of extremity probes NE, the number of tests NT (i.e. the number of pairs of initial boundary probes) and the resulting number of blocking probes NB including the two initial probes are given in Table 3. The total number of test was 11869. For all tests, the flow section was a single connected closed flow section.

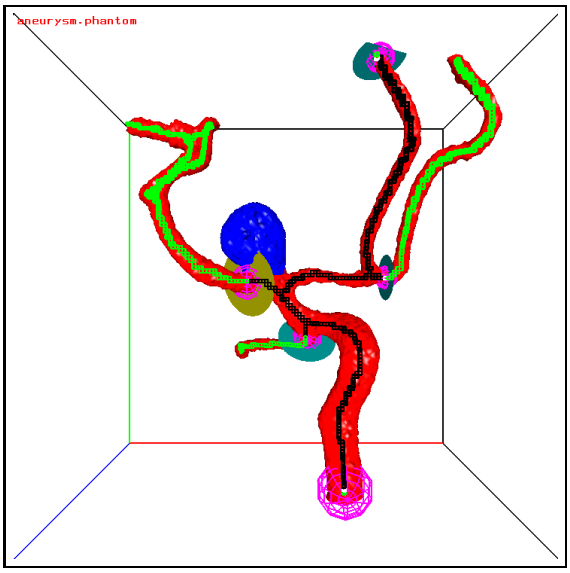

Figure 16: The closed flow section for probes 1 and 3. The skeleton voxels of the flow section are black, the other skeleton voxels are green.

Table 3: The characteristics of the number of extremity probes *NE*, the number of tests *NT* and the resulting number of blocking probes *NB* including the two initial probes for fully-automatic geometry closure of 11869 open flow sections

	NE	*NT*	*NB*
min.	3.0	3.0	3.0
median	15.5	112.5	14.0
mean	19.2	247.3	14.8
max.	56.0	1540.0	48.0

8 CONCLUSIONS

The following conclusions can be drawn from the results, the figures and the experiences gathered during testing:

1. Fully-automatic geometry closure of an aneurysm gives always correct (i.e. a single connected closed flow section) and visually acceptable results.
2. Fully-automatic geometry closure of an open flow section gives correct and visually acceptable results except when multiple closed flow sections arise from the initial boundary probes.
3. Preparing patient specific geometries for computational fluid dynamics is a time-consuming and error-prone task. The work above is the first to automatically create and validate an error free closed simulation domain. It has been implemented in a simulation and visualization software environment that allows a user to prepare a simulation in a matter of minutes instead of an hour of work.
4. Whether flow sections, generated by fully-automatic geometry closure of an aneurysm based on a length criterion, are suitable for hemodynamics simulations has yet to be investigated.

REFERENCES

Bruijns, J. (2001). Fully-automatic branch labelling of voxel vessel structures. In *Proc. VMV*, pages 341–350, Stuttgart, Germany.

Bruijns, J., Peters, F., Berretty, R., and Barenbrug, B. (2007). Fully-automatic correction of the erroneous border areas of an aneurysm. In *Proc. BVM*, pages 293–297, Muenchen, Germany.

Bruijns, J., Peters, F., Berretty, R., van Overveld, C., and ter Haar Romeny, B. (2005). Computer-aided treatment planning of an aneurysm: The connection tube and the neck outline. In *Proc. VMV*, pages 265–272, Erlangen, Germany.

Butty, V., Gudjonsson, K., P.Buchel, Makhijani, V., Ventikosa, Y., and D.Poulikakos (2002). Residence times and basins of attraction for a realistic right internal carotid artery with two aneurysms. *Biorheology*, 39:387–393.

Castro, M., Putman, C., and Cebral, J. (2005). Computational modeling of cerebral aneurysms in arterial networks reconstructed from multiple 3d rotational angiography images. In *Proc. SPIE: Medical Imaging, volume 5746*, pages 233–244, San Diego, CA, USA.

Cebral, J., Castro, M., Millan, D., Frangi, A., and Putman, C. (2005). Pilot clinical investigation of aneurysm rupture using image-based computational fluid dynamics models. In *Proc. SPIE: Medical Imaging, volume 5746*, pages 245–256, San Diego, CA, USA.

Moret, J., Kemkers, R., de Beek, J. O., Koppe, R., Klotz, E., and Grass, M. (1998). 3D rotational angiography: Clinical value in endovascular treatment. *Medicamundi*, 42(3):8–14.

Philips-Medical-Systems-Nederland (2001). INTEGRIS 3D-RA. instructions for use. release 2.2. Technical Report 9896 001 32943, Philips Medical Systems Nederland, Best, The Netherlands.

Venugopal, P., Duckwiler, G., Valentino, D., Chen, H., Villablance, P., Vinuela, F., Kemkers, R., and Haas, H. (2005). Correlating aneurysm growth to hemodynamic parameters: the case of a patient-specific anterior communicating artery aneurysm. In *Proc. SPIE: Medical Imaging, volume 5746*, pages 780–791, San Diego, CA, USA.

Waechter, I., Bredno, J., Hermans, R., Weese, J., Barratt, D., and Hawkes, D. (2008). Evaluation of model-based blood flow quantification from rotational angiography. In *Proc. SPIE: Medical Imaging, volume 6916*, San Diego, CA, USA.